Baicalein suppresses growth of non-small cell lung carcinoma by targeting MAP4K3

Jian Li [a], Lijun Yan [a,*], Jianghan Luo [a,1], Li Tong [b,1], Yuan Gao [a], Wei Feng [c], Fuling Wang [a], Wenyu Cui [a], Siming Li [a], Zhiwei Sun [a]

[a] School of Pharmacy, Institute of Cell and Molecular Biology, Harbin University of Commerce, Harbin 150076, China
[b] Gene Engineering and Biotechnology Beijing Key Laboratory, Department of Biochemistry and Molecular Biology, Beijing Normal University, Beijing 100875, China [c] National Laboratory of Biomacromolecules, Institute of Biophysics, Chinese Academy of Sciences, Beijing 100101, China

ARTICLEINFO

Keywords:
Baicalein
Non-small cell lung carcinoma
MAP4K3
Transcription factor EB
Autophagy

ABSTRACT

Exploring key genes associated with non-small cell lung carcinoma (NSCLC) may lead to targeted therapies for NSCLC patients. The protein kinase MAP4K3 has been established as an important modulator of cell growth and autophagy in mammals. Herein, we investigated the somatic mutations and the expression pattern of *MAP4K3* detected in NSCLC patients based on the TCGA database. Abnormal *MAP4K3* expression and its somatic mutations are associated with the carcinogenesis and thereby becoming an attractive therapeutic target. Baicalein, a natural product, was determined to be the first-reported MAP4K3 binding ligand with its K_D values of 6.47 μM measured by microscale thermophoresis. Subsequent *in silico* docking and mutation studies demonstrated that baicalein directly binds to MAP4K3, presumably to the substrate-binding pocket of this kinase domain, causing inactivity of MAP4K3. We further showed that baicalein could induce degradation of MAP4K3 through decreasing its stability and promoting the ubiquitin proteasome pathway. Degradation of MAP4K3 could cause dissociation of the transcription factor EB and 14-3-3 complex, enhance rapid transport of TFEB to the nucleus and trigger TFEB-dependent autophagy, resulting in lung cancer cells proliferation arrest. Knockdown of MAP4K3 expression by siRNA was sufficient to mimic baicalein-induced autophagy. Ectopic expression of the MAP4K3 protein resulted in significant resistance to baicalein-induced autophagy. Baicalein exhibited good tumor growth inhibition in a nude mouse model for human H1299 xenografts, which might be tightly related to its binding to MAP4K3 and degradation of MAP4K3. Our data provide novel mechanistic insights of baicalein/ MAP4K3/ mTORC1/ TFEB axis in regulating baicalein-induced autophagy in NSCLC, suggesting potential therapies for treatment of NSCLC.

1. Introduction

Non-small cell lung carcinoma (NSCLC) is the most common and aggressive tumor, and is one of the major causes of cancer death in the world. There are many treatments for NSCLC, including surgical resection, chemotherapy, radiotherapy, and small molecule targeted therapy and immunotherapy [1–3]. Since the seminal discovery of activating epidermal growth factor receptor gene (EGFR) mutations in 2004 [4,5], a better understanding of the fields of lung cancer-related signaling pathways enabled the development of targeted therapies that heralded the era of personalized medicine. Although EGFR tyrosine kinase inhibitor (TKI) drugs such as gefitinib are effective in NSCLC that harbor specific mutations in the tyrosine kinase domain of EGFR, acquired resistance inevitably limits the curative effects of EGFR-TKIs. The most common acquired resistance mechanisms were of three types: target gene modification, alternative pathway activation and histological or phenotypic transformation [6,7]. Therefore, it is imperative to develop new drugs and combination therapies for NSCLC treatment.

Aberrant signaling cascades emanating from EGFR are involved in the complex network of oncogenic pathways in NSCLC [8–10]. NSCLC response to EGFR TKI therapy may involve activation of Beclin 1 and autophagy [11]. PI3K, Akt, and mTOR as the downstream targets of EGFR, are well-established negative regulators of autophagy [12]. Initiation of autophagy begins with activation of the ULK1 complex [13, 14]. The mTORC1 signaling directly controls autophagy activity through the phosphorylation and inhibition of Unc-51-like kinase 1 (ULK1, also known as ATG1) [15]. The ULK1 complex induces vesicle nucleation of the autophagosome which is then mediated by a class III phosphoinositide 3-kinase (PI3K) complex containing Beclin 1/Atg 6 [16,17]. However, the oncogene Akt inhibits autophagy independently of mTOR signaling

Abbreviations: BA, Baicalein; NSCLC, non-small cell lung carcinoma; MAP4K3, mitogen activated protein kinase kinase kinase kinase 3; mTOR, mammalian target of rapamycin; TFEB, transcription factor EB; Msn, Misshapen; SQSTM1/ P62, sequestosome 1; HEK, human embryonic kidney; FBS, fetal bovine serum; CTX, cyclophosphamide; MBP, myelin basic protein; PNBM, p-nitrobenzyl mesylate; CQ, chloroquine; CHX, cycloheximide; DMSO, dimethyl sulfoxide; MST, microscale thermophoresis; siRNA, small interfering RNA; SDs, standard deviations.

* Corresponding author at: School of Pharmacy, Harbin University of Commerce, 138 Tongda Street, Daoli District, Harbin, 150076, China. *E-mail addresses:* ylj@hrbcu.edu.cn, lijunyan226@163.com (L. Yan).
[1] These authors contributed equally to this paper.

https://doi.org/10.1016/j.biopha.2020.110965
Received 24 July 2020; Received in revised form 28 October 2020; Accepted 1 November 2020
Available online 6 November 2020
0753-3322/© 2020 The Authors. Published by Elsevier Masson SAS. This is an open access article under the CC BY-NC-ND license (http://creativecommons.org/licenses/by-nc-nd/4.0/).

via serine phosphorylation of the essential autophagy protein, Beclin 1 [18]. Also, active EGFR mutants interact with Beclin 1 and inhibit autophagy independently of mTOR [11]. The mTOR protein and its downstream proteins, S6K and 4E-BP1, frequently are activated in the significant proportions of NSCLC patients [19,20]. The links between mTOR signaling and autophagy remain poorly understood, particularly the role of autophagy induction in the response to suppression of mTOR signaling in NSCLC.

The protein kinase MAP4K3 (Mitogen activated protein kinase kinase kinase kinase 3, also known as GLK, germinal center-like kinase) is a member of the *Ste20*-related family and its kinase activity is stimulated by administration of amino acids, acting upstream of mTORC1 and promoting cell growth [21,22]. During amino acid sufficiency Ser170-phosphorylated MAP4K3 activates mTORC1, but that upon amino acid restriction MAP4K3 preferentially interacts with PP2A, promoting dephosphorylation of Ser170, MAP4K3 inhibition, and, subsequently, inhibition of mTORC1 signaling [23]. MAP4K3 is required for phosphorylation of the mTORC1 downstream molecules such as S6K1. Overexpression of MAP4K3 promotes the activation of S6K1 and knockdown of MAP4K3 levels causes a decrease in cell size [24]. MAP4K3 directly interacts with and phosphorylates the transcription factor EB (TFEB), retains amino acid-sufficiency-mediated TFEB in the cytoplasm, leading to inhibition of autophagy [25]. A transautophosphorylation site at Ser170 in the MAP4K3 kinase activation segment is required for MAP4K3 activity and its activation of mTORC1 signaling [23]. Besides serine phosphorylation, tyrosine phosphorylation of MAP4K3 induced by EGF stimulation in A549 lung adenocarcinoma cells has been associated with EGFR signaling [26]. Thus, MAP4K3 looks like an attractive drug target, since that inhibitors of this enzyme should switch off the mTORC1, thereby inhibit cell growth and proliferation, and promote autophagy.

Baicalein is a typical flavonoid compound derived from the root of *Scutellaria baicalensis*. It exhibits anti-inflammatory, anti-oxidative, hepatoprotective and anti-tumor effects, and other pharmacological activities [27]. Recently, the anti-cancer effects of baicalein have been proved in many cancers types including NSCLC [27–30]. However, to our knowledge no functionally molecule directly interacting with baicalein via autophagy has been identified in NSCLC treatment. It would be interesting therefore to determine the role of autophagy induced by baicalein in NSCLC. In this study, we investigated the clinical relevance of *MAP4K3* in NSCLC patients, and examined whether and how inhibition of MAP4K3/ mTOR were involved in the effect of baicalein on NSCLC *in vitro* and *in vivo*.

2. Materials and methods

2.1. Clinical data analysis

The somatic mutation analyses of *MAP4K3* on LUSC and LUAD patients were based on the TCGA database (https://cancergenome.nih. gov/) using the GDC [31]. Data for *MAP4K3* expression across tumor and normal samples, and clinical patient data from LUSC and LUAD are based on the TCGA database and publicly available at http://ualcan. path.uab.edu [32].

2.2. Cell culture, reagents and antibodies

Human H1299, A549 and HEK (human embryonic kidney)-293 T cells were obtained from the Chinese Academy of Sciences (Shanghai Institute of Biochemistry and Cell Biology, Shanghai, China). H1299 and A549 cells were cultured in RPMI-1640 medium (Gibco, Waltham, MA, USA) supplemented with 10 % (v/v) fetal bovine serum (FBS, HyClone, LA, USA), and HEK293 T cells were cultured in DMEM medium (Gibco, USA) containing 10 % FBS. All cells were grown in the presence of 100 U/mL penicillin and 100 μg/mL streptomycin (Beyotime, China), and incubated in a 5% CO_2 atmosphere at 37 °C with 95 % humidity. Cells between passage numbers 3 and 10 were used for the experiments. Baicalein, wogonin, Myelin Basic Protein (MBP) and chloroquine (CQ) were from Sigma-Aldrich (St. Louis, MO, USA). MG-132 and cycloheximide (CHX) were obtained from Selleckchem (USA). Cyclophosphamide (CTX) injection was purchased from Jiangsu Shengdi Medicine Co., Ltd. (Jiangsu, China; Specification: 0.2 g/ bottle). ATPγS and N^6- (phenethyl) ATPγS were purchased from Biolog Life Science Institute (Germany). Nuclear and Cytoplasmic Protein Extraction kit was from Invitrogen (Thermo Fisher Scientific, Rockford, IL, USA). Antibodies against phospho-p70 S6K (Thr389), p70 S6K, MAP4K3, LC3, P62, Flag, TFEB, Phospho-(Ser) 14-3-3 Binding Motif and Histone H3 were purchased from Cell Signaling Technology (Beverly, MA, USA). Antibodies against GAPDH and MAP4K3 were purchased from Signalway Antibody LLC (USA) and Abnova (USA), respectively. Antibodies against myc (9E10) was purchased from Sigma-Aldrich. Antibodies against β-actin, thiophosphate ester, and reagent PNBM (p-nitrobenzyl mesylate) were purchased from Abcam (UK). Antibody against ubiquitin was obtained from Proteintech (USA).

2.3. Plasmids

The pRK5 mycMAP4K3 and pRK5 mycMsn plasmids were gifts from Dr. Richard F Lamb at Section of Cell and Molecular Biology, Chester Beatty Laboratories, Institute of Cancer Research, London. Mutants MAP4K3-M90 G, MAP4K3-K138A, MAP4K3-I202A, MAP4K3-T203A, MAP4K3-E206A and MAP4K3-R135A in pRK5myc were obtained using a QuickChange site-directed mutagenesis kit (Stratagene). A construct expressing truncated MAP4K3 (residues 1–390) tagged with myc at the N-terminus was generated by PCR and subcloned into the pRK5 vector. All mutant and PCR-generated plasmids were verified by DNA sequencing. In order to obtain His6-tag MAP4K3, a hexahistidine (His6)-tag was inserted to N-terminal of full-length MAP4K3 in pRK5myc vector. To observe the nuclear transfer of TFEB, full-length TFEB was cloned into pEGFP-N1 plasmid. The mRFP-EGFP-LC3 plasmid was purchased from Addgene (USA). All constructs were confirmed by sequencing analysis.

2.4. In vitro kinase activity assay

Immunoprecipitated myc-tagged MAP4K3s from HEK293 T cells were incubated at 30 °C for 30 min with 5 μg of MBP as a substrate and the indicated agents in the presence of 1 mM ATPγS or N^6-(phenethyl) ATPγS as indicated, as previously described [33]. After the phosphorylation reaction, the proteins were alkylated with 2.5 mM PNBM for 2 h at room temperature and the products were analyzed by western blot analysis.

2.5. RNA interference, immunoprecipitation assays and western blot analysis

Small interfering RNA (siRNA) targeting MAP4K3-1 was purchased from Invitrogen (USA) and siRNA targeting MAP4K3-2 was chemically synthesized by GenePharma (Shanghai, China). The siRNA sequence of MAP4K3-2 is 5′-AUCGAGCUGUUGGAUAAAGTT-3′. Cells were transfected with 25 pM siRNA duplexes in 6-well plates using siRNA MAX (Invitrogen, USA) according to the manufacturer's protocol. After 48 h of transfection, the cells were harvested for analysis using western blot.

The indicated cells were transfected with exogenous mycMAP4K3, mycMAP4K3 (1–390), mycMAP4K3-M90 G or flagTFEB for 24 h and the indicated agents in10 cm culture dish, respectively. Then whole-cell extracts were lysed in immunoprecipitation buffer (IP buffer: 25 mM Hepes, pH 7.5, 150 mM NaCl, 5 mM EDTA, 1% Triton X-100 and protease inhibitors cocktail). The lysates were incubated with protein G beads (Roche) together with the antibody against myc or flag. After 3 h incubation, beads were washed three times with ice-cold IP buffer. Proteins were eluted by IP buffer. Western blot was performed as previously described [33]. The samples were resolved by 10 % SDS-PAGE and transferred to PVDF membranes, followed by immunoblotting with the indicated antibodies.

2.6. Purification of MAP4K3 protein and microscale thermophoresis (MST)

HEK293 T cells were transfected with His6-tag MAP4K3 for 24 h and then lysed with lysis buffer, followed by centrifugation. The supernatant was purified by affinity chromatography using a HiTrap HP-column (1 mL, GE Healthcare Life Sciences, USA), and further separated by size exclusion chromatography (Superdex 200, GE). The fraction with MAP4K3 kinase activity was stored in buffer containing 20 mM Hepes (pH 7.5), 300 mM NaCl, 10 % glycerol and 3 mM DTT.

Purified MAP4K3 protein samples were diluted to 20 nM in MST buffer (50 mM Tris-HCl, 150 mM NaCl, 10 mM $MgCl_2$, 0.05 % Tween- 20) containing 5% DMSO. A dilution series of baicalein (7.81×10^{-5} M–1.53×10^{-7} M) was prepared in MST buffer containing 5% DMSO and preincubated with 20 nM MAP4K3 for 10 min at room temperature in the dark. Samples were loaded into hydrophilic capillary tubes, and measured. The binding affinity of molecules was assayed using a Monolith NT. Label Free (NanoTemper Technologies GmbH, Germany).

2.7. Molecular docking

The 3-dimensional solution structures (PDB ID: 5J5T) of MAP4K3 were extracted from the RCSB protein data bank (http://www.rcsb.org) and processed by pdbfixer. Essential hydrogens and Gasteiger chargers were added to the macromolecules MAP4K3. To sample the binding site, a grid of 40 × 40 × 40 A° (in case of specific docking) with a spacing of 0.375 A° was first computed. The 3D structure of baicalein was generated by Discovery Studio Visualizer 2020 and minimized using openbabel. Docking was performed using the Lamarckian genetic algorithm provided by AutoDock 4.2 software. The results were analyzed using PyMol.

2.8. Confocal microscopy

H1299 cells were cultured on sterile coverslips for 24 h and then transfected with EGFP-TFEB using Lipofectamine 3000 (Invitrogen, USA) according to manufacturer's instructions. Then cells were treated with DMSO or 100 μM baicalein for 24 h. Cells were fixed in ice-cold methanol for 10 min. After a quick wash with PBS, cells were permeabilized with 0.5 % Triton X-100 in PBS. A drop of DAPI containing Fluoromount- G (Southern Biotech, Birmingham, AL, USA) was added to the cells, and cover glasses were then placed on microscopic glass slides. The fluorescent images were obtained by an Olympus FV3000 confocal microscope (Japan) and >30 cells were counted per condition.

2.9. Autophagy assays

H1299 cells were cultured on sterile coverslips for 24 h and then transiently transfected with mRFP-EGFP-LC3 (Addgene, USA) plasmid for 24 h by using Lipofectamine 3000 transfection reagent (Invitrogen, Carlsbad, USA) in strict accordance with the manufacturer's instructions. Cells were then treated with DMSO or 100 μM baicalein for 24 h. After a quick wash with PBS, cover glasses were then placed on microscopic glass slides. Images were processed using a fluorescence microscope (DP71, Olympus, Japan).

2.10. Transmission electron microscopy

H1299 cells were seeded in 6-well cell culture plates and incubated for 24 h, then treated with DMSO or 100 μM baicalein for 24 h. After treatment, cells were collected and fixed in 2.5 % glutaraldehyde in phosphate buffer at 4 °C for 2 h, followed by postfixation with 1% osmium tetroxide for 2 h at room temperature. The samples were dehydrated in gradient ethanol and then embedded in araldite. Ultrathin sections of 60 nm were cut on a Leica microtome and placed on copper grids and stained with uranylacetate and lead citrate. Images were processed using a HT7700 electron microscope (HITACHI, Japan). The number of autolysosomes was determined by manual counting from at least 5 different fields.

2.11. Xenograft tumor-formation assay and treatment

Female BALB/c nude mice (18− 20 g) with 6–8 weeks of age were obtained from Beijing Vital River Laboratory Animal Technology Co., Ltd. (Beijing, China). 2 × 10^6 H1299 cells in 0.2 mL of phosphate-buffered saline (PBS) were inoculated subcutaneously into the flank of the mice. One week after inoculation, mice were randomly divided into 3 groups (n = 6 for each group). For treatment, the xenograft mice were intragastrically administered with control (23 % ddH_2O, 12 % ethanol, 60 % peanuts oil and 5% Tween-80) and baicalein (80 mg/kg body weight) daily, and intraperitoneally injected with CTX (30 mg/kg body weight) every 2 days. Tumor volumes [V=π/6 × (length) × $(width)^2$] were measured by caliper every 3 days. Mice were observed for 21 days. At the end of the experiment, mice were sacrificed and tumor were harvested, weighed and paraffin-embedded. Sections of 4 μm were cut and subjected to IHC staining. Animals were maintained under specific pathogen-free conditions with natural daylight cycles (12-h light/12-h dark) at 22 °C, 55 % humidity and had free access to food and water. All animal study protocols were approved by the Institutional Animal Care and Use Committee of Harbin University of Commerce School of Pharmacy.

2.12. Statistical analysis

Data are represented as means ± standard deviations (SDs) of three independent experiments. The statistical significance was analyzed using student's *t*-test by Graph Pad Prism 8.2.1 (GraphPad Software Inc., La Jolla, CA, USA). $p < 0.05$ were considered as the significant difference.

3. Results

3.1. Somatic mutations and the expression pattern of *MAP4K3* in NSCLC patients

To assess the clinical significance of *MAP4K3* in NSCLC patients, we used the GDC Data Portal to access to DNA sequence data in The Cancer Genome Atlas (TCGA) dataset [31]. Somatic mutations for *MAP4K3* were determined from sequencing of lung squamous cell carcinoma (LUSC) and lung adenocarcinoma (LUAD) patients. *MAP4K3* was altered in 12 of 57 (21.05 %) LUSC patients and 20 of 54 (37.04 %) LUAD patients (Fig. 1A). Next, the variants were analyzed using the variant effect predictor (VEP), as presented in the TCGA database (Fig. 1B). High and moderate impact variants were frequently observed in both LUSC (10 of

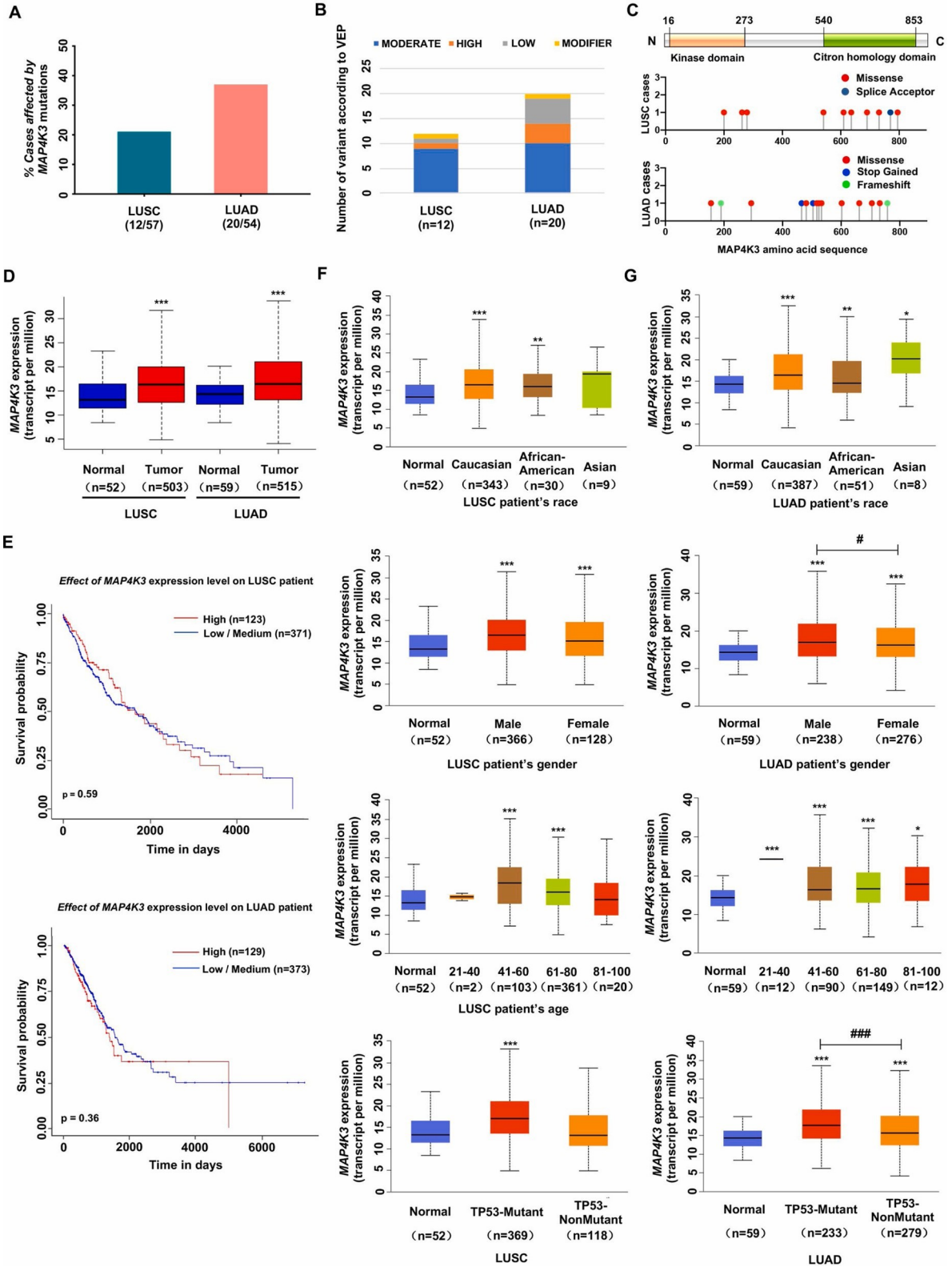

Fig. 1. Somatic mutations and the expression pattern of *MAP4K3* from LUSC and LUAD patients in the TCGA database (GDC). (A) The number of total somatic mutations of *MAP4K3.* (B) The histogram showing variant type of *MAP4K3* per individual case and number of variant according to variant effect predictor (VEP). (C) The somatic mutation distribution over MAP4K3 protein. (D) Boxplot showing relative expression of *MAP4K3* in normal and primary tumor samples. (E) Kaplan- Meier plots showing the association of *MAP4K3* expression levels with LUSC and LUAD patient survival. (F-G) Boxplot showing relative expression of *MAP4K3* in normal, LUSC and LUAD samples in subgroups based on patient's race, gender, age and TP53 mutation. Data are mean ±SD. *$p < 0.05$, **$p < 0.01$, ***$p < 0.001$ compared with the normal. #$p < 0.05$, ###$p < 0.001$ compared with the indicated subgroup.

12, 83.33 %) and LUAD (14 of 20, 70 %) patients affected by somatic mutations for *MAP4K3* (Fig. 1C).

Further examination the expression pattern of *MAP4K3* across both LUSC and LUAD primary tumors

showed high transcription of *MAP4K3* in the TCGA database (Fig. 1D, $p < 0.001$). In survival analysis, patients with high *MAP4K3* had shorter overall survival (OS) than did those with low/medium *MAP4K3* expression in both LUSC and LUAD patients. However, the duration of OS of low/medium and high *MAP4K3* expression groups did not differ significantly (Fig. 1E). Further subgroup analyses of multiple clinicopathological features for LUSC and LUAD samples in the TCGA database revealed differential transcriptional expression patterns of *MAP4K3* (Fig. 1F-G). For LUSC patients, there were significant associations between high transcription of *MAP4K3* and TP53-mutant (Fig. 1F, $p < 0.001$). The transcription level of *MAP4K3* was significantly higher in LUAD patients than healthy people in subgroup analyses based on patient's race, gender, age and TP53 mutation status (Fig. 1G, $p < 0.001$, $p < 0.01$ and $p < 0.05$). The results led to the suggestion that MAP4K3 was involved in the carcinogenesis of LUSC and LUAD patients, thereby becoming an attractive therapeutic target.

3.2. Baicalein attenuates in vitro MAP4K3 kinase activities

We next screened whether baicalein was an inhibitor specific for MAP4K3. MAP4K3 contains an N-terminal kinase domain, a central region containing tandem polyproline motifs, and a C-terminal citron homology (CNH) domain (Fig. 1C). Wildtype (WT) full-length MAP4K3 and the N-terminal kinase region (aa 1–390) were overexpressed in HEK293 T (Fig. 2A). *In vitro* kinase activities of MAP4K3 were measured by incubating the indicated baicalein and the generic substrate MBP with immunoprecipitated myc-tagged WT MAP4K3 and aa 1–390 from HEK293 T cells in the presence of ATPγS, respectively. Baicalein exerted strongly inhibitory effect on MAP4K3 kinase activities of both WT and aa

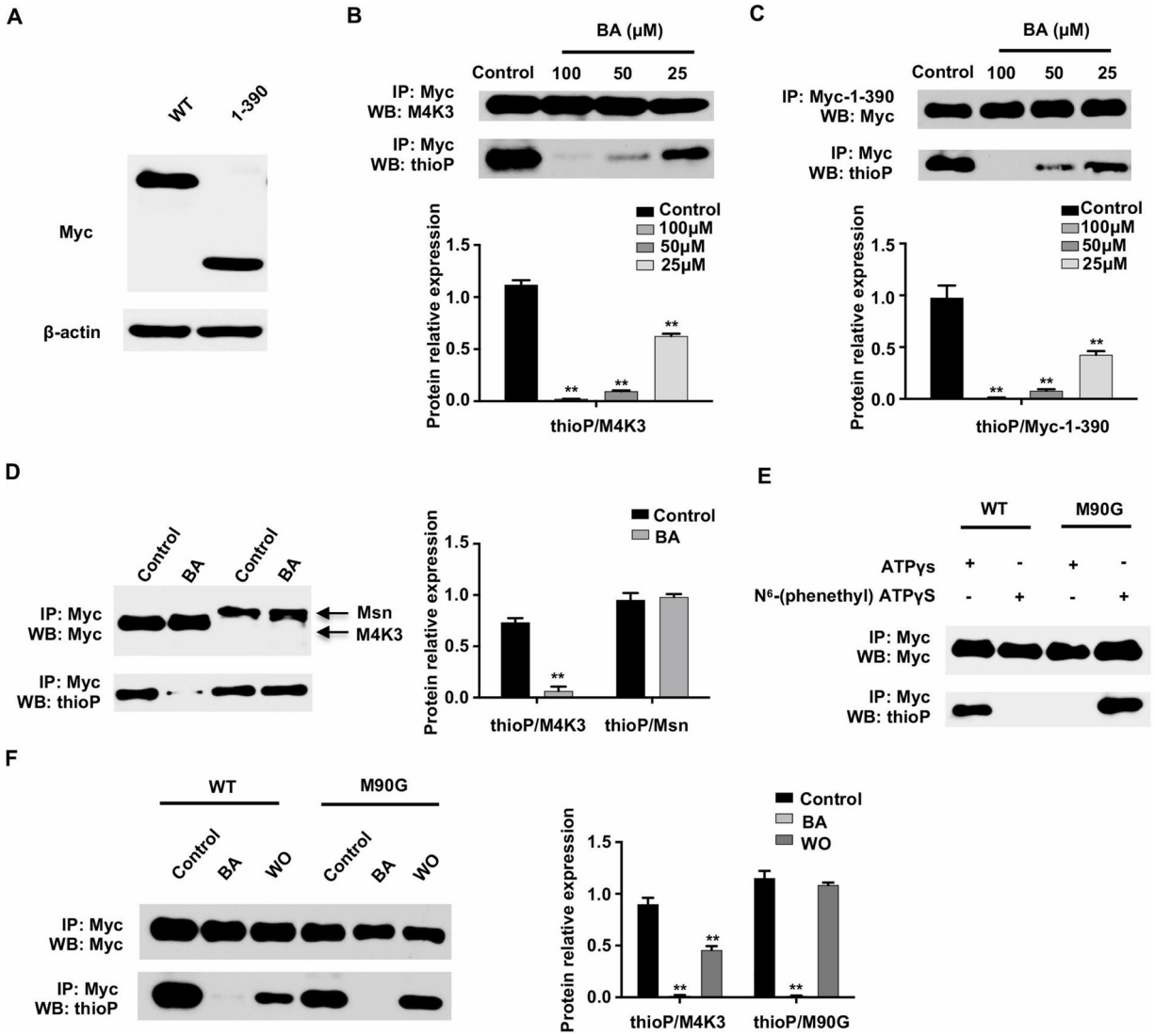

Fig. 2. Baicalein inhibits MAP4K3 kinase activity. (A) HEK293 T cells were transfected with 20 μg pRK5myc MAP4K3 and 10 μg pRK5myc 1-390 constructs and protein levels determined by immunoblotting with 9E10 antibody. (B-C) *In vitro* kinase (IVK) assays using myc-tagged MAP4K3 or myc-tagged 1-390 immunoprecipitated from HEK293 T cells with MBP as a substrate, ATPγS as a phospho-donor and the indicated concentrations of baicalein (BA) incubated at 30˚C for 30 min. Immunoblots are shown detecting phosphorylation level of MBP. (D) IVK assays of myc-tagged MAP4K3 or myc-tagged Msn immunoprecipitated from HEK293 T cells by 100 μM BA. Immunoblots are shown detecting phosphorylation level of MBP substrate. (E) IVK assays using myc-tagged MAP4K3 or myc-tagged M90 G immunoprecipitated from HEK293 T cells with MBP as a substrate and the indicated ATPγS or N^6-(phenethyl) ATPγS as a phospho-donor. Immunoblots are shown detecting phosphorylation level of MBP. (F) IVK assays using myc-tagged MAP4K3 or myc-tagged M90 G immunoprecipitated from HEK293 T cells by 100 μM BA and 100 μM wogonin (WO) with MBP as a substrate. ATPγS and N^6-(phenethyl) ATPγS as a phospho-donor for MAP4K3 and M90 G, respectively. Immunoblots are shown detecting phosphorylation level of MBP. $^{**}p < 0.01$ compared with the control group. Data are presented as mean ± SD of three independent experiments.

1–390 in a dose-dependent manner *in vitro* (Fig. 2B-C), whereas it had no inhibitory effect on the kinase activity of related control *Ste20* family kinase Msn (Fig. 2D).

Given the potential interaction between the N-terminal kinase domain and baicalein, we further asked if baicalein was a competitive ATP-binding site inhibitor of MAP4K3. The gatekeeper residue is a conserved bulky hydrophobic amino acid present at the base of the ATP- binding pocket in all typical protein kinases. Replacement of this gatekeeper residue with a smaller amino acid enables the mutant protein kinase to use ATP analogs containing bulky groups. To rule this out and confirm MAP4K3 as the target, we mutated the gatekeeper residue of MAP4K3 (methionine 90) to glycine residue (MAP4K3 M90 G). We then tested the *in vitro* kinase activity of WT MAP4K3 and MAP4K3 M90 G in the presence of ATPγS or a variety of ATPγS containing bulky groups. MAP4K3 M90 G was able to use N6-(phenethyl) ATPγS to phosphorylate MBP but used ATPγS to a lesser extent than WT-MAP4K3 (Fig. 2E). Thus, methionine 90 is the gatekeeper residue in MAP4K3. Moreover, mutation of this residue to a glycine did not prevent baicalein-mediated inhibition of MAP4K3 activity (Fig. 2F), though it changed the ATP binding properties of the kinase. In contrast, wogonin had no inhibitory effect on the *in intro* kinase activity of MAP4K3 M90 G, though it was shown to reduce kinase activity of WT MAP4K3 to a lesser extent than

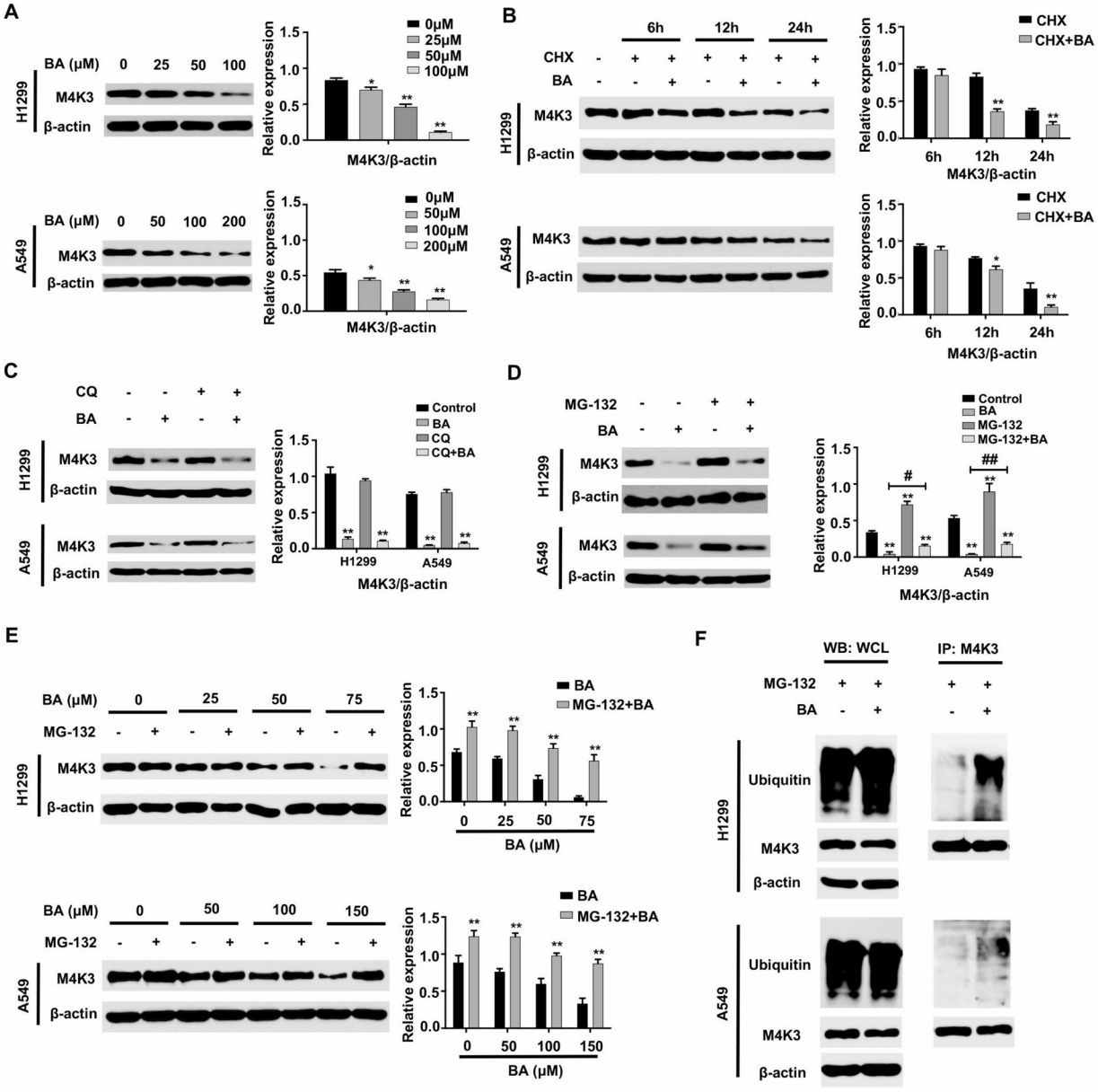

Fig. 3. Baicalein inhibits MAP4K3 protein expression through decreasing its stability and increasing degradation. (A) H1299 and A549 cells were treated with indicated concentrations of baicalein (BA) for 24 h, respectively. The expression levels of MAP4K3 (M4K3) were examined by western blot analysis. (B) Malignant cells were treated with 25 μg/mL cycloheximide (CHX) in the absence or presence of 100 μM BA (for H1299 cells) or 200 μM BA (for A549 cells) for different times. The expression of MAP4K3 protein was detected by western blot. Malignant cells were treated without or with 20 μM CQ (C) or 5 μM MG-132 (D) pre-incubated for 0.5 h in the presence of 100 μM BA (for H1299 cells) or 200 μM BA (for A549 cells). After 24 h treatment, cell lysates were subjected to western blot analysis. (E) H1299 and A549 cells were treated with the indicated concentrations of BA in the absence or presence of 5 μM MG-132 for 24 h. The expression levels of MAP4K3 (M4K3) was examined by western blot analysis. *p <0.05, **p <0.01 compared with the control group, #p < 0.05, ##p < 0.01 in comparison with BA group and combination group. Data are presented as mean ± SD of three independent experiments. (F) Representative results of immunoprecipitation after treatment malignant cells with 5 μM MG-132 in the absence or the presence of 75 μM (for H1299 cells) and 150 μM BA (for A549 cells). After 24h treatment, cell lysates were immunoprecipitated with anti-MAP4K3 antibody, followed by western blot analysis with anti-ubiquitin antibody. Data are presented from three independent experiments.

baicalein (Fig. 2F). These results indicated that baicalein was unlikely to be a competitive ATP-binding site inhibitor of MAP4K3.

3.3. Baicalein inhibits MAP4K3 protein expression through decreasing its stability and increasing degradation

We first examined the expression levels of MAP4K3 in NSCLC cell lines A549 and H1299 following baicalein treatment. Western blot analysis revealed that baicalein markedly reduced the endogenous expression of MAP4K3 (Fig. 3A). To determine whether this was secondary to alterations in protein stability, both A549 and H1299 cells were treated with cycloheximide (CHX) and baicalein for 6 h, 12 h, 24 h. The results showed that baicalein treatment in the presence of CHX reduced the de novo synthesis of MAP4K3 protein more rapidly than CHX treatment alone (Fig. 3B), indicating that baicalein decreased the stability of MAP4K3 protein.

An alternative possibility was that the downregulations of MAP4K3 protein expression is the result of baicalein-involved a proteasome-dependent or lysosome-dependent mechanism. To test this, we examined the effect of the proteasome inhibitor, MG-132, or the inhibitor of lysosomal acidification, CQ on MAP4K3 protein level in both A549 and H1299 cells. CQ could not rescue the already existing MAP4K3 protein or the loss of MAP4K3 in response to baicalein in both A549 and H1299 cells (Fig. 3C). However, the already existing MAP4K3 protein could be rescued by MG-132, but MG-132 can only rescue the loss of MAP4K3 in response to baicalein in both A549 and H1299 cells to a lesser extent (Fig. 3D). To further confirm that MG132 rescued baicalein-induced degradation of MAP4K3 protein, both A549 and H1299 cells were exposed to MG132 (5 μM) or /and the indicated concentrations of baicalein. The results showed baicalein promoted proteasome-dependent degradation of MAP4K3 in both cells (Fig. 3E), confirming that the hypothesis of MG132 effect at MAP4K3 protein level. Furthermore, increased accumulation of baicalein-induced MAP4K3 tagged with ubiquitin was observed when MG132 inhibited proteasome activity, indicating that baicalein promoted proteasome- dependent degradation of MAP4K3 in both A549 and H1299 cells (Fig. 3F).

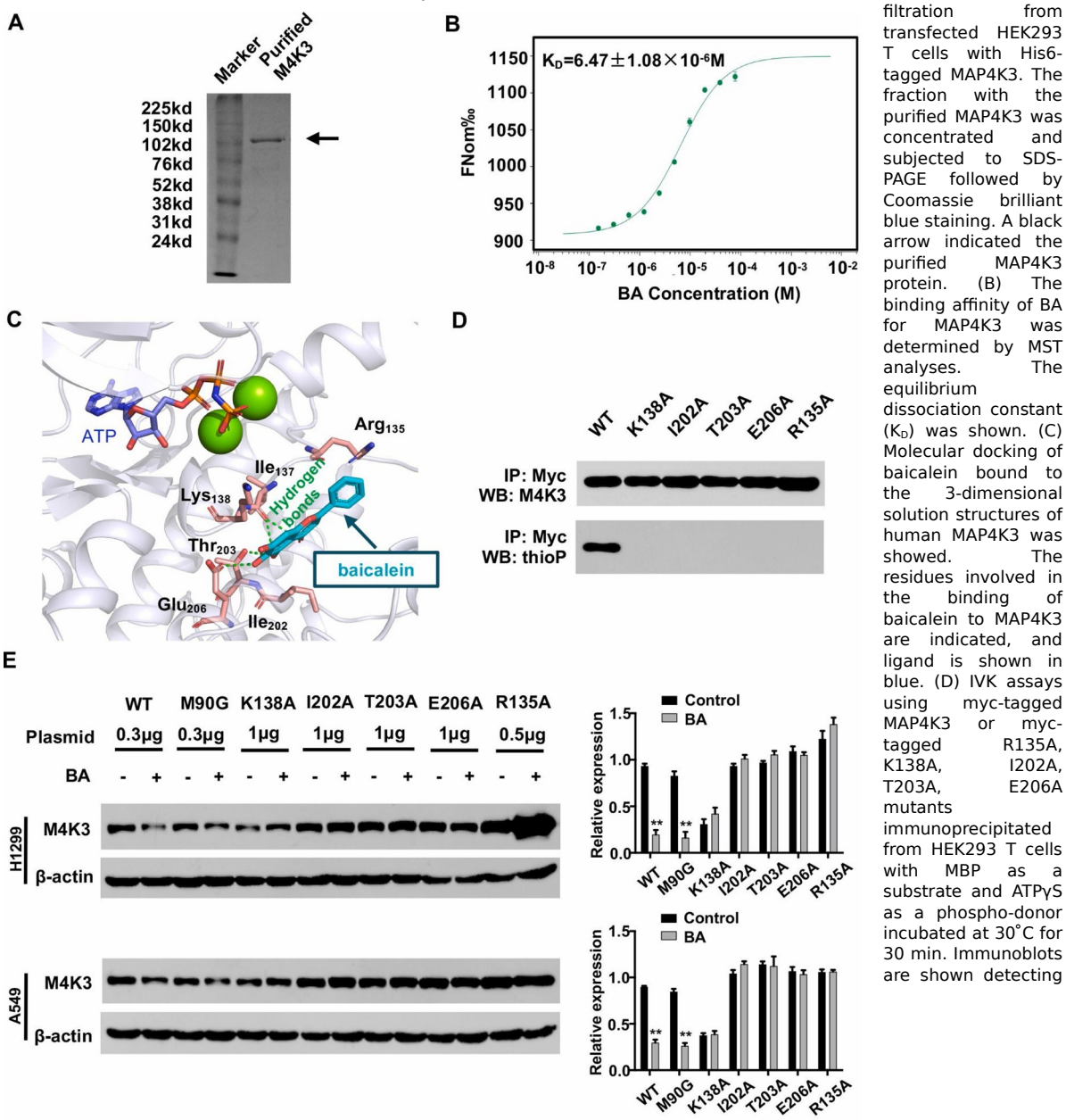

Fig. 4. Baicalein directly binds to MAP4K3. (A) MAP4K3 protein was prepared by affinity chromatography and gel filtration from transfected HEK293 T cells with His6-tagged MAP4K3. The fraction with the purified MAP4K3 was concentrated and subjected to SDS-PAGE followed by Coomassie brilliant blue staining. A black arrow indicated the purified MAP4K3 protein. (B) The binding affinity of BA for MAP4K3 was determined by MST analyses. The equilibrium dissociation constant (K_D) was shown. (C) Molecular docking of baicalein bound to the 3-dimensional solution structures of human MAP4K3 was showed. The residues involved in the binding of baicalein to MAP4K3 are indicated, and ligand is shown in blue. (D) IVK assays using myc-tagged MAP4K3 or myc-tagged R135A, K138A, I202A, T203A, E206A mutants immunoprecipitated from HEK293 T cells with MBP as a substrate and ATPγS as a phospho-donor incubated at 30˚C for 30 min. Immunoblots are shown detecting

phosphorylation level of MBP. (E) Malignant cells were transfected with indicated amount of mycMAP4K3 or myc-tagged K138A, I202A, T203A, E206A, R135A for 24 h, then malignant cells were treated with 100 μM BA (for H1299 cells) or 200 μM BA (for A549 cells) for 24 h. The expression levels of MAP4K3 (M4K3) and β-actin were examined by western blot analysis. $^{**}p < 0.01$ compared with the control group. Data are presented as mean ± SD of three independent experiments.

3.4. Baicalein directly binds to MAP4K3

To better understand the molecular mechanism of action of baicalein, we used microscale thermophoresis (MST) to characterize the baicalein and MAP4K3 interaction. The full-length WT MAP4K3 proteins were purified to near-homogeneity (Fig. 4A). Then, we mixed the purified MAP4K3 with serial dilutions of baicalein or a structurally related flavone, wogonin, so as to evaluate the affinity of baicalein for MAP4K3 via MST. We obtained an equilibrium dissociation constant K_D of 6.47 ± 1.08 μM in the label-free approach (Fig. 4B), indicating a high affinity between baicalein and the protein kinase MAP4K3. However, the resulting binding between wogonin and MAP4K3 couldn't be achieved under the same equilibrium conditions (data not shown).

To further define the interaction between baicalein and MAP4K3, an *in silico* molecular docking study with baicalein on the 3-dimensional solution structures of human MAP4K3 was performed. We hypothesized that baicalein occupied the polypeptide binding site so that MAP4K3 cannot self-phosphorylate and further phosphorylate its other substrates. The baicalein-binding site was predicted to consist of 6 residues using PyMol. Baicalein not only formed hydrogen bonds with Ile137, Thr203 and Glu206, but also formed the van der Waals interactions with Lys138, Arg135 and Ile202 (Fig. 4C). It is worth noting that baicalein only forms a hydrogen bond interaction with the amino acid main chain of Ile137, and interacts with the side chains of the other five amino acids. The docking analysis suggests that the effect of baicalein in reducing kinase activity is likely due to its effect in reducing substrate binding affinity. To further confirm the binding effect, we generated a panel of mutations in which all five residues known to be bound to baicalein were mutated to alanine. We tested the *in vitro* kinase activity of WT MAP4K3 and MAP4K3 T203A, E206A, K138A, R135A and I202A, respectively. Unlike WT MAP4K3, none of the MAP4K3 mutants were able to phosphorylate MBP (Fig. 4D). One possibility was that these baicalein-binding sites of MAP4K3 are important to the polypeptide binding. We then examined whether the degradation of MAP4K3 occurred via baicalein binding or other indirect results. To distinguish these possibilities, we asked whether baicalein didn't reduce the expression of MAP4K3 mutants. Upon transient transfection of WT MAP4K3 and its mutants into both A549 and H1299 cells, all mutants expression were no longer inhibited by baicalein in cells (Fig. 4E), suggesting that MAP4K3 T203, E206, K138, R135 and I202 are primarily baicalein-binding site.

3.5. Baicalein regulates TFEB subcellular localization in a MAP4K3- dependent manner

Next, we asked whether degradation of MAP4K3 by baicalein activated TFEB via promoting its nuclear translocation. We then performed quantification of TFEB levels in the cytosolic and nuclear fractions by

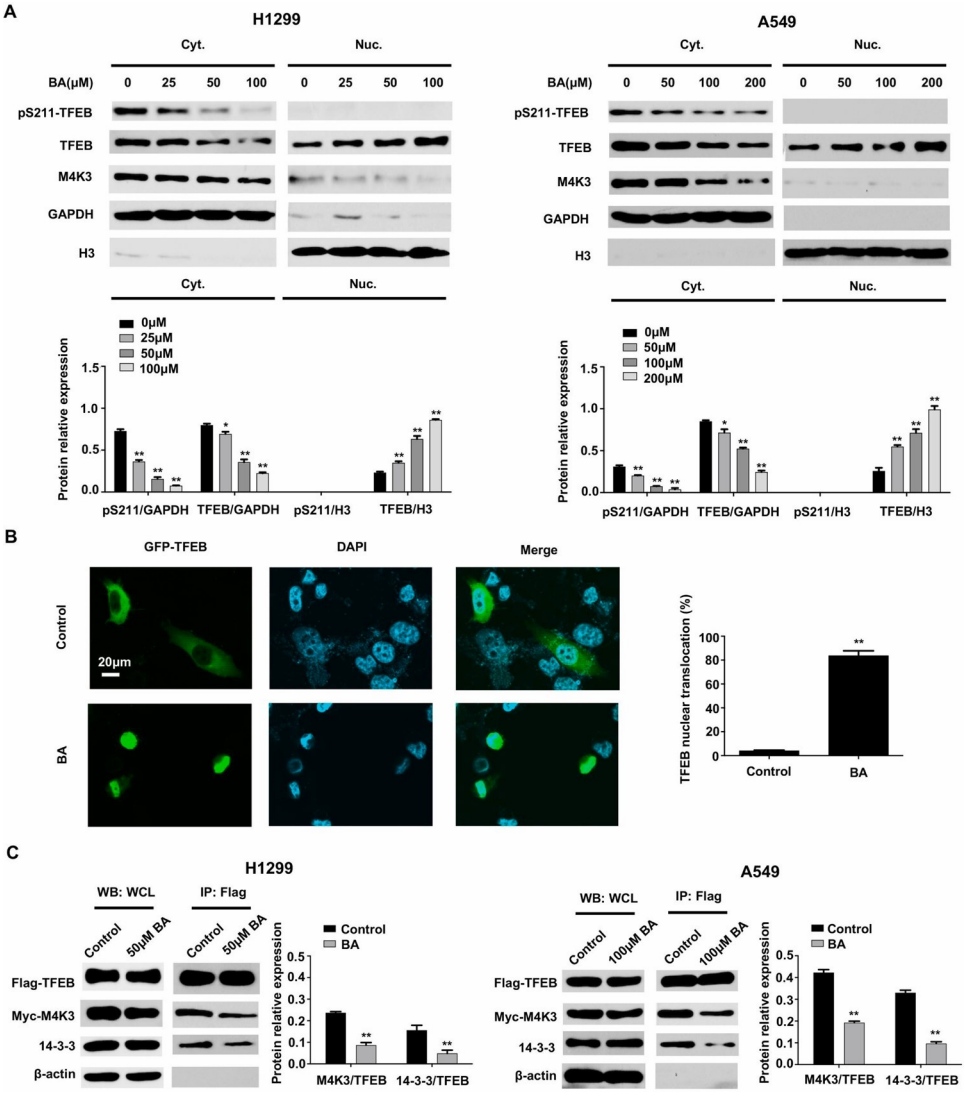

Fig. 5. Baicalein induces the nuclear translocation of TFEB in a MAP4K3-dependent manner. (A) H1299 and A549 cells were transfected with flagTFEB for 24 h, then cells were treated with indicated concentrations of baicalein (BA) for 24 h. The expression levels of pS211-TFEB, TFEB and MAP4K3 in the cytosolic (Cyt.) and nuclear (Nuc.) fractions were determined by western blotting. GAPDH and histone H3 were used as loading controls of the cytoplasmic and nuclear fraction, respectively. An antibody against the specific YWHA/ 14-3-3 motif was used to recognize the expression level of pS211-TFEB. (B) H1299 cells were transfected with GFP-TFEB for 24 h and treated with 100 μM BA or DMSO for 24 h. Images were processed by an Olympus FV3000 confocal microscope. Quantification of cells with predominantly TFEB nuclear localization from experiment shown. n > 30 cells per condition. Scale bar represents 20 μm. (C) H1299 and A549 cells were transfected with flagTFEB and mycMAP4K3 for 24 h, and treated with the indicated concentrations of BA or DMSO for 24 h. MycMAP4K3 and endogenous 14-3-3 were coimmunoprecipitated with flagTFEB. The levels of immunoprecipitated MAP4K3 and 14-3-3 were normalized to their corresponding levels in whole cell lysates (WCL), *p <0.05, **p <0.01 compared with the control group. Data are presented as mean ± SD of three independent experiments.

western blots. TFEB redistributed from the cytosol to the nucleus in response to baicalein in a dose-dependent manner, indicating that baicalein could activate nuclear translocation of TFEB in both A549 and H1299 cells (Fig. 5A). Nuclear transfer of GFP-TFEB was also observed by confocal microscopy. When TFEB localized to the cytosol in control cells overexpressing GFP-TFEB, however, TFEB no longer localized to the cytosol but instead mostly remained in the nucleus (more than 80 % cells) after baicalein treatment (Fig. 5B). In both A549 and H1299 cells overexpressing TFEB and MAP4K3, both levels of 14-3-3 and MAP4K3 coimmunoprecipitated with flagTFEB obviously decreased after baicalein treatment compared with the control (Fig. 5C). Degradation of MAP4K3 by baicalein resulted in dissociation of the TFEB/14-3-3 complex which appeared to require MAP4K3 kinase activity, suggesting that baicalein could cause dissociation of

the TFEB/14-3-3 complex in a MAP4K3-dependent manner and further promote TFEB nuclear translocation where it functioned lysosomal biogenesis and autophagy.

3.6. Knockdown of MAP4K3 expression by siRNA is sufficient to mimic baicalein-induced autophagy

MAP4K3 activates mTOR signaling to S6K. We further observed that baicalein treatment markedly reduced the phosphorylation of S6K at Thr389, increased the expression of LC3-II and decreased the expression of P62 in a dose-dependent manner in malignant cells (Fig. 6A). In comparison, we performed a siRNA knockdown experiment on MAP4K3 using both A549 and H1299 cells as a model system. Specific knockdown of MAP4K3 expression (using either the M4K3-1 or M4K3-2 siRNAs) markedly increased the expression of LC3-II and reduced the expression of P62 [34], indicating that inhibition of MAP4K3 can mediate the autophagy of both cell lines (Fig. 6B). To further examine the role of MAP4K3 in baicalein-mediated autophagy, MAP4K3 was introduced into both A549 and H1299 cells by transient transfection of plasmids expressing the MAP4K3 protein. Ectopic expression of the MAP4K3 protein resulted in significant resistance to baicalein-induced autophagy (Fig. 6C)

Subsequently, we identified an increased number of autolysosomes in baicalein-treated malignant cells via electron microscopy (Fig. 6D). Also, we further observed that baicalein treatment significantly increased the number of mRFP-GFP-LC3 dots representing both autophagosomes and autolysosomes per cell, indicating that baicalein could induce autophagy and enhance autophagic flux (Fig. 6E-F).

3.7. Baicalein inhibits NSCLC growth in vivo

To evaluate the therapeutic effect of baicalein, we measured the growth rate of tumor and size of tumor in a nude mouse model for human H1299 xenografts. As shown in Fig. 7A-C, either baicalein treatment or CTX treatment significantly reduced the volumes and weights of tumors compared with that of the model control, demonstrating the anti-tumor effects of baicalein *in vivo*. Subsequently, the results of immunohistochemistry showed that the level of MAP4K3 expression was much lower in baicalein administration group compared with those in the model control (Fig. 7D). This was further confirmed by examination of tumor tissues via western blot analysis. Baicalein treatment led to a higher LC3-II expression and a lower P62 protein expression in tumor tissues (Fig. 7E).

4. Discussion

Exploration of the large samples numbers in TCGA is imperative to unearth novel therapeutic/diagnostic biomarkers [31,32]. Of the 111 cases with sequencing data, about 21.62 % (24 of 111) patients in both LUSC and LUAD had somatic mutations in *MAP4K3* including frameshift variants, splice acceptor variants, stop gained variants and missense variants, which might lead to abnormal mRNA or protein expression levels of MAP4K3 or its functional impairment. A *MAP4K3* somatic mutation at E351 K has been identified in human pancreatic cancer, and this mutant transgenic mouse line (PolII-GLKE351 K Tg) expressed a constitutively activated GLK (E351 K) mutant [35,36]. We found that the expression of *MAP4K3* was significantly higher in 1018 cases of both LUSC and LUAD patients than healthy people. Unlike EGFR gene mutations/overexpression in NSCLC patients [37], our data showed that LUAD patients with higher *MAP4K3* levels were more commonly men than women, which was consistent with a previous report on MAP4K3 protein overexpression [38]. High *MAP4K3* expression was independent of patient's race and age in both LUAD and LUSC patients. However, the association between *MAP4K3* expression and patient's race and age may be underestimated due to the small sample size of patients (only 2.36 % Asian and 0.41 % age (21–40) in LUSC patients; only 1.79 % Asian and 4.56 % age (21–40 or 81–100) in LUAD patients). Our data suggested that MAP4K3 is an oncogene involved in the carcinogenesis of LUSC and LUAD patients.

Little is known about the regulation of MAP4K3 ubiquitination and degradation. In this study, we found that baicalein induced the degradation of MAP4K3 through decreasing its stability and promoting proteasome-dependent mechanisms in malignant cells. We demonstrate that MAP4K3 is a direct target of baicalein. MST, *in silico* docking and mutation studies further support baicalein directly binding to MAP4K3, presumably to the substrate-binding pocket rather than ATP-binding site. Wogonin, a structurally related natural flavone, could reduce kinase activity of WT MAP4K3 to a lesser extent than baicalein. This indication is further supported by the fact that we could not detect binding of MAP4K3 to wogonin in MST assay. Since wogonin is a competitive ATP-binding site inhibitor of CDK9 and RIPK1 [39,40], it had no inhibitory effect on M90 G activity when mutation of this residue to a glycine changed the ATP binding properties of MAP4K3. In addition, baicalein did not inhibit the activity of other members of the *Ste20* family, for example, Msn. The results indicated that baicalein preferentially inhibited the kinase activity of MAP4K3 and degraded its protein in malignant cells.

Several lines of evidence indicate that upregulated MAP4K3 function contributes to NSCLC metastasis / recurrence [36,38,41]. Our data showed MAP4K3 overexpression in NSCLC xenograft tumors. Thus, downregulation of MAP4K3 proteins may facilitate the development of novel targeted therapies for NSCLC. In this study, baicalein could induce autophagy in NSCLC xenograft tumors and malignant cells, and enhance autophagic flux, which was consistent with a previous report [42]. Of note, specific knockdown of MAP4K3 expression by RNA interference is sufficient to mimic baicalein-induced autophagy. We confirmed by knockdown and overexpression experiments that MAP4K3 is an important modulator of autophagy and a key survival factor for tumors. Thus, MAP4K3, which is efficiently targeted by baicalein, would also be beneficial for diseases including multiple types of cancer, neurodegenerative disorders, lysosomal storage diseases, and possibly autoimmune disorders [25].

TFEB is a member of the basic helix–loop–helix leucine zipper family of transcription factors that controls lysosomal biogenesis, lysosomal acidification, lysosomal exocytosis and autophagy [43]. Under normal nutrient conditions, TFEB is phosphorylated at Ser211 in an mTORC1-dependent manner. This phosphorylation promotes association of TFEB with members of the YWHA /14-3-3 family of proteins and retention of the transcription factor in the cytosol [44]. MAP4K3 at serine 3 phosphorylation of TFEB occurs before and is necessary for TFEB serine 211 phosphorylation by mTORC1 [25]. In this study, baicalein could inhibit MAP4K3, reduce S6K1 Thr389 phosphorylation and TFEB serine 211 phosphorylation, cause dissociation of the TFEB/ 14-3-3 complex and activate TFEB via promoting its nuclear translocation in both A549 and H1299 cells, which might be tightly related to its binding to MAP4K3 and degradation of MAP4K3.

A recent study indicated the role of AMPK/Drp1/mitochondrial fission axis in regulating baicalein-induced apoptosis and autophagy in lung cancer [42]. It is evident that the mechanism by which baicalein

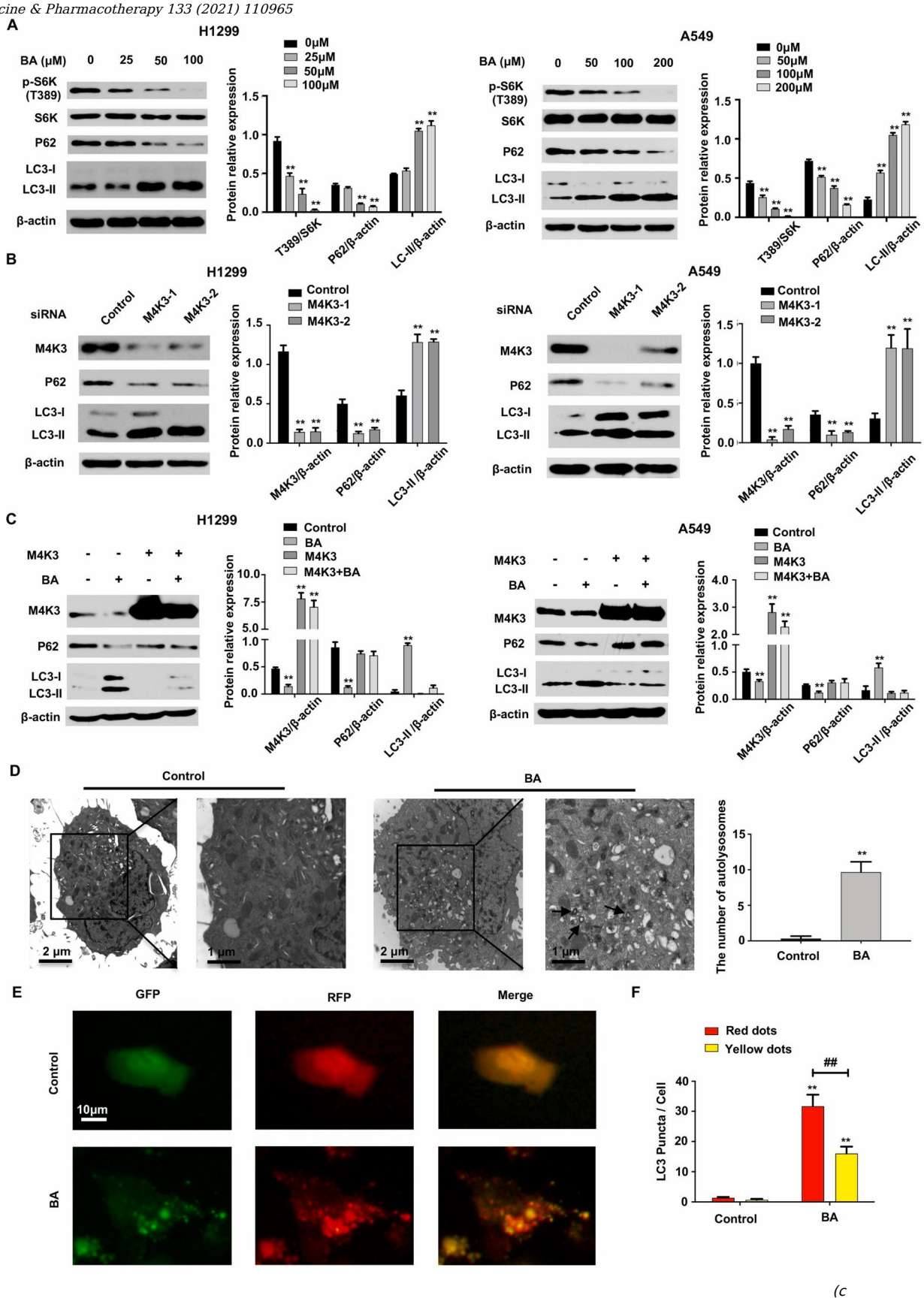
A
H1299
BA (μM) 0 25 50 100
p-S6K (T389)
S6K
P62
LC3-I
LC3-II
β-actin
0μM
25μM
50μM
100μM
Protein relative expression
T389/S6K
P62/β-actin
LC-II/β-actin
A549
BA (μM) 0 50 100 200
0μM
50μM
100μM
200μM
B
siRNA Control M4K3-1 M4K3-2
M4K3
M4K3/β-actin
LC-II /β-actin
C
M4K3 - - + +
BA - + - +
Control
BA
M4K3
M4K3+BA
D
Control
BA
2 μm
1 μm
The number of autolysosomes
E
GFP
RFP
Merge
10μm
F
Red dots
Yellow dots
##
LC3 Puncta / Cell

(caption on

next page)

Fig. 6. Knockdown of MAP4K3 is sufficient to mimic bai cal ei n-induced autophagy. (A) H1299 and A549 cells were tre

ated with the indicated concentrations of BA for 24 h. The phosphorylation level of S6K and the expression levels of LC3, P62 were

xamined by western blot analysis. β-actin was used as the loading control. (B) H1299 and A549 cells were transfected with either two dist

inct siRNA duplexes (M4K3-1 and M4K3-2) targeting MAP4K3 or scrambled siRNA as control. After 48 h, the expression levels of LC3, P

62 and MAP4K3 were examined by western blot analysis. β-actin was used as the loading control. (C) H1299 and A549 cells were tra

nsfected with or without the MAP4K3 expressing plasmid (M4K3) for 24 h, then cells were treated with 100 μM BA or DMSO for 24 h. The e

x
pr
es
si
o
n
le
v
el
s
of
M
A
P
4
K
3,
L
C
3
a
n
d
P
6
2
w
er
e
e
x
a
m
in
e
d
b
y
w
es
te
rn
bl
ot
a
n
al
ys
is.
β-
a
ct
in
w
as
us
e
d
as
th
e
lo
a
di
n
g
c
o
nt
ro
l.
(
D
)
R
e
pr
es

entative transmission electron microscopy images of H1299 cells after treatment with vehicle or 100 μM BA for 24 h. Black arrows indic

ated autolysosomes. The number of autolysosomes was determined by manual counting from at least 5 different fields. Scale bar, 2 μm

(left) and 1 μm (right). (E) H1299 cells were transfected with mRFP-GFP-LC3 for 24 h and treated with DMSO or 100 μM BA for another

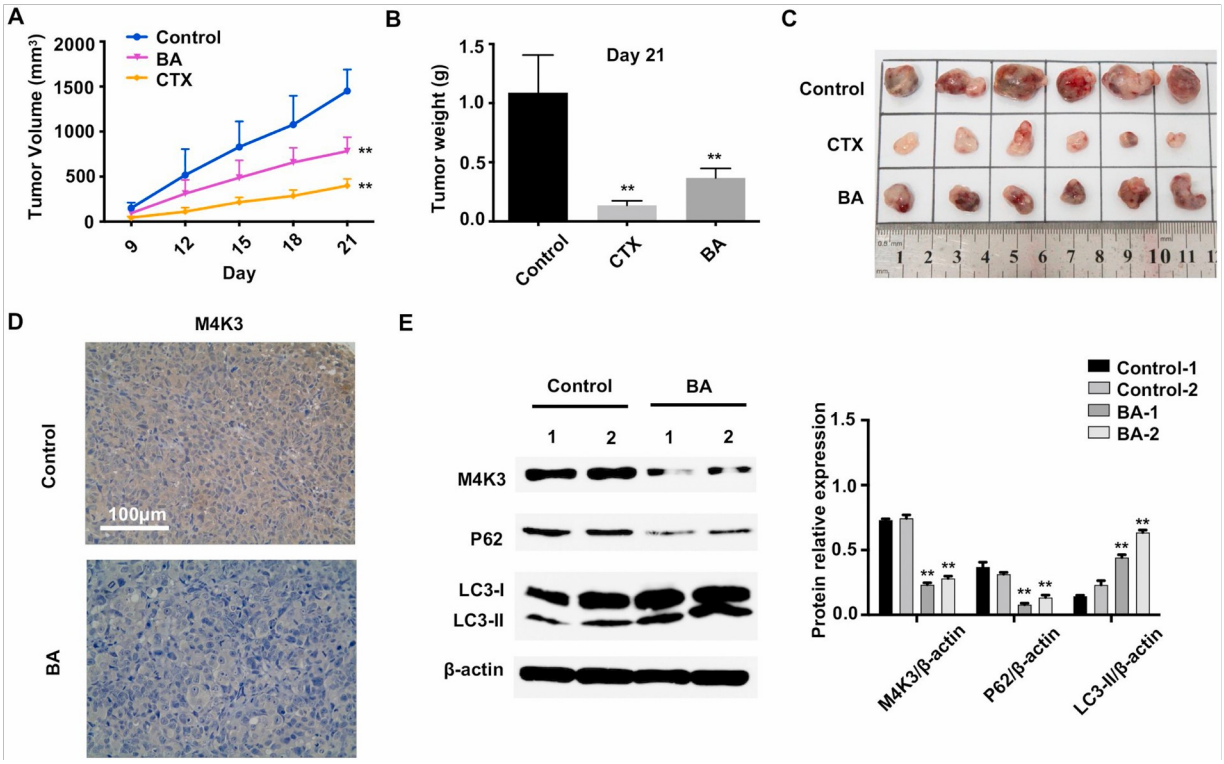

Fig. 7. Baicalein inhibited NSCLC growth *in vivo*. (A-B) H1299 xenograft mice were randomly into control, CTX and BA group. Tumor volumes were measured every 3 days, and tumor weights were recorded at day 21 (n =6). (C) Representative images of tumors. (D) Representative IHC staining images of MAP4K3 were performed in the 2 groups of tumor samples. Scale bar represents 100 μm. (E) The expression levels of MAP4K3 (M4K3), P62 and LC3 in tumor tissues were examined by western blot analysis. $^{**}p$ <0.01 compared with the control group. Data are presented as mean ± SD of three independent experiments.

increases ULK1 and AMPK phosphorylation at Ser 555 and Thr 172, How baicalein acts upstream of both AMPK/ULK1 and MAP4K3/mrespectively, and reduces inhibitory phosphorylation on Ser 757 of TOR/ULK1 axis needs to be studied further. The first task is to identify ULK1 in cancer cells [45]. ULK1 is phosphorylated at different sites by autophagy-related substrates of ULK1 complex, but it remains as an multiple kinases, including AMPK, mTOR and protein kinase B [46]. open question [47,48].

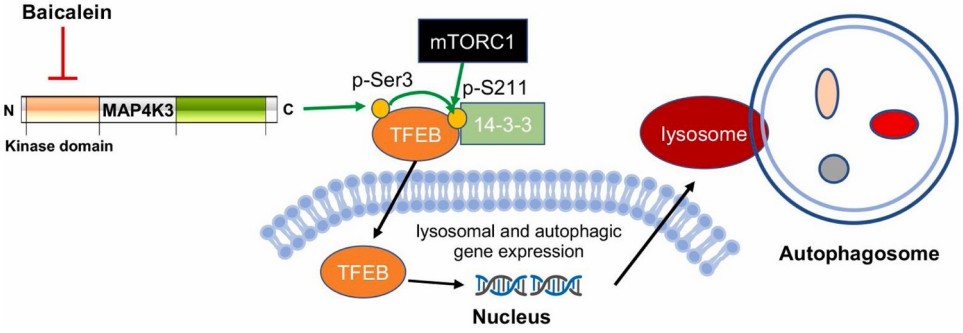

Fig. 8. Schematic representation of the hypothesized molecular mechanism underlying MAP4K3 inhibition by baicalein. Baicalein directly regulated MAP4K3, a critical enzyme for the mTOR upstream, to trigger transcription factor EB-dependent autophagy initiation, cause dissociation of the TFEB/ 14-3-3 complex and enhance rapid transport of TFEB to the nucleus, resulting in enhanced autophagy and NSCLC cells proliferation arrest.

In conclusion, the somatic mutations and the expression pattern of *MAP4K3* revealed that MAP4K3 is an oncogene involved in the carcinogenesis of NSCLC patients based on the TCGA database. We functionally characterized baicalein, a natural product, that suppressed growth in human NSCLC xenograft tumors and malignant cells through inducing autophagy. Our data was the first to reveal a good affinity between MAP4K3 and baicalein, and the mechanism of MAP4K3 degradation induced by baicalein. Baicalein causes dissociation of the TFEB/14-3-3 complex in a MAP4K3-dependent manner, resulting in promoting its nuclear translocation of TFEB, triggering TFEB-dependent autophagy initiation and NSCLC cells proliferation arrest (Fig. 8). Together, our data provide novel

mechanistic insights of baicalein/ MAP4K3/ mTORC1/ TFEB axis in regulating baicalein-induced autophagy in NSCLC, suggesting that baicalein is a potential therapeutic drug for NSCLC patients.

CRediT authorship contribution statement

Jian Li: Investigation, Formal analysis, Methodology, Visualization, Data curation. **Lijun Yan:** Conceptualization, Investigation, Formal analysis, Methodology, Writing - original draft, Writing - review & editing, Supervision, Funding acquisition. **Jianghan Luo:** Resources, Project administration. **Li Tong:** Resources, Project administration. **Yuan Gao:** Validation. **Wei Feng:** Resources, Project administration. **Fuling Wang:** Resources, Project administration. **Wenyu Cui:** Validation. **Siming Li:** Validation. **Zhiwei Sun:** Validation.

Declaration of Competing Interest

The authors declare no potential conflicts of interest.

Acknowledgments

We thank Dr. Richard F Lamb at Section of Cell and Molecular Biology, Chester Beatty Laboratories, Institute of Cancer Research, London, for the gift of the pRK5mycWT-MAP4K3 and Msn plasmids and Prof. Qun Wei at Department of Biochemistry and Molecular Biology, Beijing Normal University, Beijing, for helpful discussion. This work was supported by grants for the National Natural Science Foundation of China (Grant No. 31370764), the Natural Science Foundation of Heilongjiang Province (Grant No. ZD2015007, and Grant No. LH2020C059), and Department of Education of Heilongjiang Province (Grant No. TSTAU-R2018011).

Appendix A. Supplementary data

Supplementary material related to this article can be found, in the online version, at doi:https://doi.org/10.1016/j.biopha.2020.110965.

References

[1] L.A. Torre, F. Bray, R.L. Siegel, J. Ferlay, J. Lortet-Tieulent, A. Jemal, Global cancer statistics, 2012, CA Cancer J. Clin. 65 (2) (2015) 87–108. http://10.3322/caac .21262.
[2] F. Bray, J. Ferlay, I. Soerjomataram, R.L. Siegel, L.A. Torre, A. Jemal, Global cancer statistics 2018: GLOBOCAN estimates of incidence and mortality worldwide for 36 cancers in 185 countries, CA Cancer J. Clin. 68 (6) (2018) 394–424. http://10.3322/caac.21492.
[3] R.S. Herbst, D. Morgensztern, C. Boshoff, The biology and management of non- small cell lung cancer, Nature 553 (7689) (2018) 446–454. http://10.1038/na ture25183.
[4] T.J. Lynch, D.W. Bell, R. Sordella, S. Gurubhagavatula, R.A. Okimoto, B.
W. Brannigan, P.L. Harris, S.M. Haserlat, J.G. Supko, F.G. Haluska, D.N. Louis, D. C. Christiani, J. Settleman, D.A. Haber, Activating mutations in the epidermal growth factor receptor underlying responsiveness of non-small-cell lung cancer to gefitinib, N. Engl. J. Med. 350 (21) (2004) 2129–2139. http://10.1056/NEJ Moa040938.
[5] J.G. Paez, P.A. Janne, J.C. Lee, S. Tracy, H. Greulich, S. Gabriel, P. Herman, F. J. Kaye, N. Lindeman, T.J. Boggon, K. Naoki, H. Sasaki, Y. Fujii, M.J. Eck, W.
R. Sellers, B.E. Johnson, M. Meyerson, EGFR mutations in lung cancer: correlation with clinical response to gefitinib therapy, Science 304 (5676) (2004) 1497–1500. http://10.1126/science.1099314.
[6] S.G. Wu, J.Y. Shih, Management of acquired resistance to EGFR TKI-targeted therapy in advanced non-small cell lung cancer, Mol. Cancer 17 (1) (2018) 38, https://doi.org/10.1186/s12943-018-0777-1.
[7] X. Zhu, L. Chen, L. Liu, X. Niu, EMT-mediated acquired EGFR-TKI resistance in NSCLC: mechanisms and strategies, Front. Oncol. 9 (2019) 1044, https://doi.org/10.3389/fonc.2019.01044.
[8] M. Soda, Y.L. Choi, M. Enomoto, S. Takada, Y. Yamashita, S. Ishikawa, S. Fujiwara,
H. Watanabe, K. Kurashina, H. Hatanaka, M. Bando, S. Ohno, Y. Ishikawa, H. Aburatani, T. Niki, Y. Sohara, Y. Sugiyama, H. Mano, Identification of the transforming EML4-ALK fusion gene in non-small-cell lung cancer, Nature 448 (7153) (2007) 561–566. http://10.1038/nature05945.
[9] F. Facchinetti, G. Rossi, E. Bria, J.C. Soria, B. Besse, R. Minari, L. Friboulet, M. Tiseo, Oncogene addiction in non-small cell lung cancer: focus on ROS1 inhibition, Cancer Treat. Rev. 55 (2017) 83–95. http://10.1016/j.ctrv.2017.02.010
.
[10] C. Fumarola, M.A. Bonelli, P.G. Petronini, R.R. Alfieri, Targeting PI3K/AKT/mTOR pathway in non small cell lung cancer, Biochem. Pharmacol. 90 (3) (2014) 197–207. http://10.1016/j.bcp.2014.05.011.
[11] Y. Wei, Z. Zou, N. Becker, M. Anderson, R. Sumpter, G. Xiao, L. Kinch, P. Koduru,
C.S. Christudass, R.W. Veltri, N.V. Grishin, M. Peyton, J. Minna, G. Bhagat, B. Levine, EGFR-mediated Beclin 1 phosphorylation in autophagy suppression, tumor progression, and tumor chemoresistance, Cell 154 (6) (2013) 1269–1284. http://10.1016/j.cell.2013.08.015.
[12] J. Botti, M. Djavaheri-Mergny, Y. Pilatte, P. Codogno, Autophagy signaling and the cogwheels of cancer, Autophagy 2 (2) (2006) 67–73. http://10.4161/auto .2.2.2458.
[13] J.M.M. Levy, C.G. Towers, A. Thorburn, Targeting autophagy in cancer, Nat. Rev. Cancer 17 (9) (2017) 528–542. http://10.1038/nrc.2017.53.
[14] N. Mizushima, T. Yoshimori, Y. Ohsumi, The role of Atg proteins in autophagosome formation, Annu. Rev. Cell Dev. Biol. 27 (2011) 107–132. http://10.1146/annure v-cellbio-092910-154005.
[15] V.W. Rebecca, R.K. Amaravadi, Emerging strategies to effectively target autophagy in cancer, Oncogene 35 (1) (2016) 1–11. http://10.1038/onc.2015.99.
[16] Y. Ohsumi, Historical landmarks of autophagy research, Cell Res. 24 (1) (2014) 9–23. http://10.1038/cr.2013.169.
[17] O.F. F, T.E. Rusten, H. Stenmark, Phosphoinositide 3-kinases as accelerators and brakes of autophagy, FEBS J. 280 (24) (2013) 6322–6337. http://10.1111/f ebs.12486.
[18] R.C. Wang, Y. Wei, Z. An, Z. Zou, G. Xiao, G. Bhagat, M. White, J. Reichelt, B. Levine, Akt-mediated regulation of autophagy and tumorigenesis through Beclin 1 phosphorylation, Science 338 (6109) (2012) 956–959. http://10.1126/science.1 225967.
[19] Y. Dobashi, S. Suzuki, H. Matsubara, M. Kimura, S. Endo, A. Ooi, Critical and diverse involvement of Akt/mammalian target of rapamycin signaling in human lung carcinomas, Cancer 115 (1) (2009) 107–118. http://10.1002/cncr.23996.
[20] Y. Dobashi, S. Suzuki, M. Kimura, H. Matsubara, H. Tsubochi, I. Imoto, A. Ooi, Paradigm of kinase-driven pathway downstream of epidermal growth factor receptor/Akt in human lung carcinomas, Hum. Pathol. 42 (2) (2011) 214–226. http://10.1016/j.humpath.2010.05.025.
[21] M. Resnik-Docampo, J.F. de Celis, MAP4K3 is a component of the TORC1 signalling complex that modulates cell growth and viability in Drosophila melanogaster, PLoS One 6 (1) (2011) e14528. http://10.1371/journal.pone.0014528.
[22] L. Yan, R.F. Lamb, Signalling by amino acid nutrients, Biochem. Soc. Trans. 39 (2) (2011) 443–445. http://10.1042/BST0390443.
[23] L. Yan, V. Mieulet, D. Burgess, G.M. Findlay, K. Sully, J. Procter, J. Goris, V. Janssens, N.A. Morrice, R.F. Lamb, PP2A T61 epsilon is an inhibitor of MAP4K3 in nutrient signaling to mTOR, Mol. Cell 37 (5) (2010) 633–642. http://10.1016/j.molcel.2010.01.031.
[24] G.M. Findlay, L. Yan, J. Procter, V. Mieulet, R.F. Lamb, A MAP4 kinase related to Ste20 is a nutrient-sensitive regulator of mTOR signalling, Biochem. J. 403 (1) (2007) 13–20. http://10.1042/BJ20061881.
[25] C.L. Hsu, E.X. Lee, K.L. Gordon, E.A. Paz, W.C. Shen, K. Ohnishi, J. Meisenhelder, T. Hunter, A.R. La Spada, MAP4K3 mediates amino acid-dependent regulation of autophagy via phosphorylation of TFEB, Nat. Commun. 9 (1) (2018) 942. http ://10.1038/s41467-018-03340-7.

[26] D.E. Hammond, R. Hyde, I. Kratchmarova, R.J. Beynon, B. Blagoev, M.J. Clague, Quantitative analysis of HGF and EGF-dependent phosphotyrosine signaling networks, J. Proteome Res. 9 (5) (2010) 2734–2742. http://10.1021/pr100145w.
[27] T. Zhao, H. Tang, L. Xie, Y. Zheng, Z. Ma, Q. Sun, X. Li, Scutellaria baicalensis Georgi. (Lamiaceae): a review of its traditional uses, botany, phytochemistry, pharmacology and toxicology, J. Pharm. Pharmacol. 71 (9) (2019) 1353–1369. http://10.1111/jphp.13129.
[28] B. Yang, H. Bai, Y. Sa, P. Zhu, P. Liu, Inhibiting EMT, stemness and cell cycle involved in baicalin-induced growth inhibition and apoptosis in colorectal cancer cells, J. Cancer 11 (8) (2020) 2303–2317. http://10.7150/jca.37242.
[29] H. Lian, Y. Hui, T. Xiaoping, T. Wei, X. Jiyi, Y. Xiaolan, Baicalein suppresses the proliferation of human cervical cancer cells via Notch 1/Hes signaling pathway, J. Cancer Res. Ther. 15 (6) (2019) 1216–1220. http://10.4103/0973-1482.204 899.
[30] Z.H. Liu, C.X. Yang, L. Zhang, C.Y. Yang, X.Q. Xu, Baicalein, as a Prooxidant, Triggers Mitochondrial Apoptosis in MCF-7 Human Breast Cancer Cells Through Mobilization of Intracellular Copper and Reactive Oxygen Species Generation, Onco Targ. Ther. 12 (2019) 10749–10761. http://10.2147/OTT.S222819.
[31] R.L. Grossman, A.P. Heath, V. Ferretti, H.E. Varmus, D.R. Lowy, W.A. Kibbe, L.
M. Staudt, Toward a shared vision for Cancer Genomic data, N. Engl. J. Med. 375
(12) (2016) 1109–1112. http://10.1056/NEJMp1607591.
[32] D.S. Chandrashekar, B. Bashel, S.A.H. Balasubramanya, C.J. Creighton, I. Ponce- Rodriguez, B.V.S.K. Chakravarthi, S. Varambally, UALCAN: a portal for facilitating tumor subgroup gene expression and survival analyses, Neoplasia 19 (8) (2017) 649–658. http://10.1016/j.neo.2017.05.002.
[33] Y. Zhou, T. Hong, L. Tong, W. Liu, X. Yang, J. Luo, F. Wang, J. Li, L. Yan, Astragalus polysaccharide combined with 10-hydroxycamptothecin inhibits metastasis in non- small cell lung carcinoma cell lines via the MAP4K3/mTOR signaling pathway, Int. J. Mol. Med. 42 (6) (2018) 3093–3104. http://10.3892/ijmm.2018.3868.
[34] D.J. Klionsky, K. Abdelmohsen, A. Abe, et al., Guidelines for the use and interpretation of assays for monitoring autophagy (3rd edition), Autophagy 12 (1) (2016) 1–222. http://10.1080/15548627.2015.1100356.
[35] S. Jones, X. Zhang, D.W. Parsons, J.C. Lin, R.J. Leary, P. Angenendt, P. Mankoo,
H. Carter, H. Kamiyama, A. Jimeno, S.M. Hong, B. Fu, M.T. Lin, E.S. Calhoun,
M. Kamiyama, K. Walter, T. Nikolskaya, Y. Nikolsky, J. Hartigan, D.R. Smith,
M. Hidalgo, S.D. Leach, A.P. Klein, E.M. Jaffee, M. Goggins, A. Maitra,
C. Iacobuzio-Donahue, J.R. Eshleman, S.E. Kern, R.H. Hruban, R. Karchin, N. Papadopoulos, G. Parmigiani, B. Vogelstein, V.E. Velculescu, K.W. Kinzler, Core signaling pathways in human pancreatic cancers revealed by global genomic analyses, Science 321 (5897) (2008) 1801–1806. http://10.1126/science.11 64368.
[36] H.C. Chuang, C.C. Chang, C.F. Teng, C.H. Hsueh, L.L. Chiu, P.M. Hsu, M.C. Lee, C. P. Hsu, Y.R. Chen, Y.C. Liu, P.C. Lyu, T.H. Tan, MAP4K3/GLK promotes lung Cancer metastasis by phosphorylating and activating IQGAP1, Cancer Res. 79 (19) (2019) 4978–4993. http://10.1158/0008-5472.CAN-19-1402.
[37] G. da Cunha Santos, F.A. Shepherd, M.S. Tsao, EGFR mutations and lung cancer, Annu. Rev. Pathol. 6 (2011) 49–69. http://10.1146/annurev-pathol-011110-1 30206.
[38] C.P. Hsu, H.C. Chuang, M.C. Lee, H.H. Tsou, L.W. Lee, J.P. Li, T.H. Tan, GLK/ MAP4K3 overexpression associates with recurrence risk for non-small cell lung cancer, Oncotarget 7 (27) (2016) 41748–41757. http://10.18632/oncotarget .9410.
[39] G. Polier, J. Ding, B.V. Konkimalla, D. Eick, N. Ribeiro, R. Kohler, M. Giaisi, ¨
T. Efferth, L. Desaubry, P.H. Krammer, M. Li-Weber, Wogonin and related natural flavones are inhibitors of CDK9 that induce apoptosis in cancer cells by transcriptional suppression of Mcl-1, Cell Death Dis. 2 (7) (2011) e182-e182, http://10.1038/cddis.2011.66.
[40] X.-M. Meng, H.-D. Li, W.-F. Wu, P.M.-K. Tang, G.-L. Ren, L. Gao, X.-F. Li, Y. Yang, T. Xu, T.-T. Ma, Z. Li, C. Huang, L. Zhang, X.-W. Lv, J. Li, Wogonin protects against cisplatin-induced acute kidney injury by targeting RIPK1-mediated necroptosis, Lab. Investig. 98 (1) (2018). http://10.1038/labinvest.2017.115.
[41] B. Zhao, H. Han, J. Chen, Z. Zhang, S. Li, F. Fang, Q. Zheng, Y. Ma, J. Zhang, N. Wu, Y. Yang, MicroRNA let-7c inhibits migration and invasion of human non-small cell lung cancer by targeting ITGB3 and MAP4K3, Cancer Lett. 342 (1) (2014) 43–51. http://10.1016/j.canlet.2013.08.030.
[42] X. Deng, J. Liu, L. Liu, X. Sun, J. Huang, J. Dong, Drp1-mediated mitochondrial fission contributes to baicalein-induced apoptosis and autophagy in lung cancer via activation of AMPK signaling pathway, Int. J. Biol. Sci. 16 (8) (2020) 1403–1416. http://10.7150/ijbs.41768.
[43] M. Sardiello, M. Palmieri, A. di Ronza, D.L. Medina, M. Valenza, V.A. Gennarino,
C. Di Malta, F. Donaudy, V. Embrione, R.S. Polishchuk, S. Banfi, G. Parenti, E. Cattaneo, A. Ballabio, A gene network regulating lysosomal biogenesis and function, Science 325 (5939) (2009) 473–477. http://10.1126/science.1174447.
[44] J.A. Martina, Y. Chen, M. Gucek, R. Puertollano, MTORC1 functions as a transcriptional regulator of autophagy by preventing nuclear transport of TFEB, Autophagy 8 (6) (2012) 903–914. http://10.4161/auto.19653.
[45] P. Aryal, K. Kim, P.H. Park, S. Ham, J. Cho, K. Song, Baicalein induces autophagic cell death through AMPK/ULK1 activation and downregulation of mTORC1 complex components in human cancer cells, FEBS J. 281 (20) (2014) 4644–4658. http://10.1111/febs.12969.
[46] M. Bach, M. Larance, D.E. James, G. Ramm, The serine/threonine kinase ULK1 is a target of multiple phosphorylation events, Biochem. J. 440 (2) (2011) 283–291, https://doi.org/10.1042/BJ20101894.
[47] A.S. Loffler, S. Alers, A.M. Dieterle, H. Keppeler, M. Franz-Wachtel, M. Kundu, D. ¨ G. Campbell, S. Wesselborg, D.R. Alessi, B. Stork, Ulk1-mediated phosphorylation of AMPK constitutes a negative regulatory feedback loop, Autophagy 7 (7) (2011). http://10.4161/auto.7.7.15451.
[48] J. Kim, M. Kundu, B. Viollet, K.L. Guan, AMPK and mTOR regulate autophagy through direct phosphorylation of Ulk1, Nat. Cell Biol. 13 (2) (2011) 132–141. htt p://10.1038/ncb2152.